

This document was produced
by scanning the original publication.

Ce document est le produit d'une
numérisation par balayage
de la publication originale.

CANADA
DEPARTMENT OF MINES AND TECHNICAL SURVEYS
Dominion Observatories

PUBLICATIONS
of the
DOMINION OBSERVATORY
OTTAWA

Volume XXV . No. 5

DIFFUSION EFFECTS OBSERVED
IN THE WAKE SPECTRUM
OF A GEMINID METEOR

Ian Halliday

*Reprinted from Smithsonian Contributions to Astrophysics
volume 7, page 161, 1963*

Diffusion Effects Observed in the Wake Spectrum of a Geminid Meteor

By Ian Halliday¹

The spectrum of a spectacular Geminid meteor was photographed on the night of December 12/13, 1960, at the Meanook Meteor Observatory ($\varphi = 54^{\circ}37'N$, $\lambda = 113^{\circ}21'W$). This is one of two meteor observatories operated by the Dominion Observatory in northern Alberta. The spectrum exhibits interesting peculiarities.

The meteor was photographed with a converted K19 aerial camera, focal length 12 inches, focal ratio $f/2.5$, using Kodak Spectroscopic I-D emulsion on glass plates 8 by 10 inches. A Bausch & Lomb replica transmission grating with 300 lines per mm was mounted immediately in front of the camera objective. The camera was occulted 12.5 times per second by a rotating shutter with a closed-to-open ratio of 2:1.

The meteor was not observed visually but was recorded on an exposure that began at 3^h32^m U.T. and ended at 4^h05^m U.T., December 13, 1960. The meteor was initially outside the field of view of the camera, but the zero-order image entered the field before peak luminosity was attained, while the first- and second-order spectra entered the field at progressively lower heights.

The spectrum is reproduced in plate 1. The meteor moved from upper right to lower left. The right-hand edge of the photograph is the edge of the original plate. The first segment of the zero order at the top of the photograph is the sixth segment that appeared on the plate, while the lower end of the zero order (beyond segment 13) has been omitted at the left. The segment numbers are shown opposite each segment of the spectrum along the right-hand edge. Segments 20 and 21 are detectable only

in the first-order image of the Na D lines. A small portion of the first- and second-order spectra of Vega appears in the lower left corner of the photograph.

Height and velocity measures

Since the meteor was photographed from only one station, no direct measures of height or velocity are possible. Reasonably accurate heights may be obtained, however, by assuming a radiant position and velocity for the Geminid shower and then determining ranges and hence heights from the observed angular velocity.

A standard Geminid radiant at $\alpha = 113^{\circ}$, $\delta = +32^{\circ}$, was assumed (Millman, 1954) since the meteor appeared within an hour of the peak of the shower (solar longitude $261^{\circ}.1$). This assumed radiant was displaced to allow for the effect of zenith attraction. It was then found that the observed trail passed through the apparent radiant shortly before the end of the exposure, which gave a computed time for the appearance of the meteor of 4^h01^m U.T.

A plot of the observed angular velocities along the trail indicated a marked deceleration in the latter half of the observed trail. The angular velocity at the bottom of segment 4 was assumed to correspond to a meteoric velocity of 36.0 km/sec, and other heights and velocities were based on this assumption. The meteor was 90° from the radiant near the end of segment 10, at a minimum range of 106.0 km from the camera. Table 1 lists the computed heights (corrected to sea level) and corresponding velocities at the lower ends of selected segments. Errors in the assumed meteoric velocity, radiant position, and speed of shutter rotation could result in the heights and velocities of table 1

¹ Dominion Observatory, Ottawa, Canada.

being in error by as much as 3 to 5 percent. There is no doubt, however, that the meteor penetrated to unusually low heights in the atmosphere.

TABLE 1.—*Heights and velocities*

Segment	Height of bottom of segment (km)	Velocity (km/sec)
1	72.9	36.1
5	67.2	36.0
9	61.5	35.4
13	55.9	33.7
15	53.3	32.3
17	50.7	30.3
19	48.5	26.7
21	46.6	----

The meteor spectrum

The dispersions of the first and second orders of the meteor spectrum were found to be 95 and 46 Å/mm, respectively. Atomic emission lines identified in this spectrum are shown in table 2. A total of 95 features are identified. The spectrum appears normal for a meteor of this velocity except that the lines of ionized magnesium, calcium, and silicon are relatively strong compared to those in the spectra of fainter meteors with the same velocity. Almost all the lines in table 2 were also identified in a recent study of Perseid spectra (Halliday, 1961). The only significant addition is the pair of lines of Al I at 3944 and 3961 Å. These are barely detectable by sighting along the lines in a 30× enlargement of the strongest segment of the second order. The much greater relative strength of the H and K lines for fast meteors makes the detection of faint lines in this spectral region very difficult for Perseid spectra.

TABLE 2.—*Measured emission lines in the Geminid spectrum*

λ_{meas}	Atom or ion	Mult.	λ_{lab}
3683.1	Fe I	5	3679.9
			3683.1
	Fe I	21	3687.5
3705.4	Fe I	5	3705.6
			3707.8
	Fe I	21	3709.2
3719.9	Fe I	5	3719.9
3735.6	Fe I	5	3737.1
	Fe I	21	3734.9
3747.8	Fe I	5	3745.6
			3748.3
	Fe I	21	3749.5

TABLE 2.—*Measured emission lines in the Geminid spectrum—Continued*

λ_{meas}	Atom or ion	Mult.	λ_{lab}
3797.1	Fe I	21	3795.0
			3798.5
			3799.5
3815.9	Fe I	45	3815.8
3821.0	Fe I	20	3820.4
3825.1	Fe I	20	3825.9
	Fe I	45	3827.8
3832.8	Mg I	3	3829.4
			3832.3
	Fe I	20	3834.2
3839.1	Mg I	3	3838.8
3856.4	Fe I	4	3856.4
	Si II	1	3856.0
3859.7	Fe I	4	3859.9
3878.2	Fe I	4	3878.6
	Fe I	20	3878.0
3886.5	Fe I	4	3886.3
3900.3	Fe I	4	3899.7
3905.5	Fe I	4	3906.5
3921.4	Fe I	4	3920.3
			3922.9
3933.6	Ca II	1	3933.7
3943.6	Al I	1	3944.0
3960.6	Al I	1	3961.5
3968.8	Ca II	1	3968.5
	Fe I	43	3969.3
3997.2	Fe I	276	3998.1
	Fe I	278	3997.4
4005.0	Fe I	43	4005.2
4030.8	Mn I	2	4030.8
4033.5	Mn I	2	4033.1
			4034.8
4046.1	Fe I	43	4045.8
4063.4	Fe I	43	4063.6
4071.7	Fe I	43	4071.7
4132.4	Si II	3	4130.9
	Fe I	43	4132.1
4144.4	Fe I	43	4143.9
	Fe I	523	4143.4
4155.5	Fe I	354	4156.8
	Fe I	355	4154.5
4200.9	Fe I	42	4202.0
	Fe I	152	4198.3
	Fe I	522	4199.1
4217.3	Fe I	3	4216.2
4226.6	Ca I	2	4226.7
	Fe I	693	4227.4
4250.9	Fe I	42	4250.8
	Fe I	152	4250.1
4253.6	Cr I	1	4254.3
4260.6	Fe I	152	4260.5
4272.1	Fe I	42	4271.8
	Fe I	152	4271.2
4274.2	Cr I	1	4274.8
4282.2	Fe I	71	4282.4
	Ca I	5	4283.0

TABLE 2.—Measured emission lines in the Geminid spectrum—Continued

λ_{meas}	Atom or ion	Mult.	λ_{lab}
4290.2	Cr I	1	4289.7
	Ca I	5	4289.4
	Fe I	3, 41	4291.5
4307.6	Fe I	42	4307.9
	Ca I	5	4307.7
4314.2	Fe I	71	4315.1
4325.8	Fe I	42	4325.8
4353.1	Mg I	14	4351.9
	Fe I	71	4352.7
4376.1	Fe I	2	4375.9
4383.6	Fe I	41	4383.5
4404.8	Fe I	41	4404.8
4415.9	Fe I	41	4415.1
4427.1	Fe I	2	4427.3
4461.6	Fe I	2	4461.7
4481.4	Mg II	4	4481.1
			4481.3
	Fe I	2	4482.2
4530	Fe I	68	4528.6
4920.4	Fe I	318	4919.0
			4920.5
4955.1	Fe I	318	4957.3
			4957.6
5008.9 ^b	Fe I	16	5012.1
	Fe I	318	5006.1
5041.3	Fe I	16	5041.1
	Fe I	36	5041.8
5108.5	Fe I	1	5110.4
	Fe I	16	5107.5
	Fe I	36	5107.6
5146.1 ^b	Fe I	16	5142.9
			5150.8
	Fe I	383	5139.5
	Na I	8	5148.8
			5153.4
5169.4	Mg I	2	5167.3
			5172.7
	Fe I	1	5166.3
			5168.9
	Fe I	36	5171.6
	Fe I	37	5167.5
5183.6	Mg I	2	5183.6
5207.2	Cr I	7	5204.5
			5206.0
			5208.4
5227.2	Fe I	37	5227.2
	Fe I	383	5226.9
			5232.9
5269.5	Fe I	15	5269.5
	Fe I	37	5270.4
	Fe I	383	5266.6
5328.5	Fe I	15	5328.0
	Fe I	37	5328.5
5341.8	Fe I	37	5341.0
5370.5	Fe I	15	5371.5

^b Feature noticeably broad.

TABLE 2.—Measured emission lines in the Geminid spectrum—Continued

λ_{meas}	Atom or ion	Mult.	λ_{lab}
5402.8	Fe I	15	5397.1
			5405.8
5429.8	Fe I	15	5429.7
5448.8	Fe I	15	5446.9
5456.9	Fe I	15	5455.6
5499.0	Fe I	15	5497.5
			5501.5
			5506.8
5528.3	Mg I	9	5528.4
5573.2	Fe I	686	5572.9
5587.2	Fe I	686	5586.8
5615.5	Fe I	686	5615.5
5685.8	Na I	6	5682.6
			5688.2
5712	Fe I	686	5709.4
	Mg I	8	5711.1
5892.9	Na I	1	5890.0
			5895.9
5980.2	Si II	4	5979.0
6063	Fe I	207	6065.5
6105	Ca I	3	6102.7
6121.9	Ca I	3	6122.2
6139	Fe I	169	6136.6
	Fe I	207	6137.7
6157.0	Na I	5	6154.2
			6160.7
6162.7	Ca I	3	6162.2
6229	Fe I	207	6230.7
6251	Fe I	169	6252.6
6347.1	Si II	2	6347.1
6369	Si II	2	6371.4
6397.8	Fe I	168	6393.6
	Fe I	816	6400.0
6438	Ca I	18	6439.1
6461	Fe I	168	6462.7
	Ca I	18	6462.6
6494.4	Fe I	168	6495.0

Variation in luminosity

The photograph in plate 1 indicates that this meteor maintained approximately peak luminosity from segments 6 to 16, inclusive, an atmospheric path length of 27 km. Before segment 6, the zero order is considerably weaker, while the spectral lines are fading noticeably by segment 17 and drop abruptly in intensity at segment 19. Peak luminosity appears to occur at about segment 11, near a height of 59 km. The lines in the blue region of the first-order spectrum appear stronger here than in subsequent segments, although the variation between segments 11 and 14 is quite small.

To estimate the peak luminosity the zero-order image of the meteor was compared with zero-order star trails. The meteor trail is definitely weaker than the trail of Vega and appears to match the zero order of α Cygni. The meteor image trails across the plate at a rate 5,820 times greater than does the image of α Cygni, corresponding to a difference of 9.4 magnitudes. The apparent magnitude of α Cygni is +1.3, from which the meteor magnitude is estimated at -8. This is a "panchromatic" magnitude, which may be influenced by such factors as emulsion sensitivity and the blaze of the grating. In other cases (Cook and Millman, 1956; Millman and Cook, 1959), it proved to be only slightly different from photographic magnitudes.

The meteor exhibits a rapid flickering superimposed on the gradual rise and fall in overall intensity. The frequency of the flickering was estimated in each segment by measuring the fraction of a complete segment occupied by the largest number of complete cycles observed within the segment. The results were converted to cycles per second and are shown plotted in figure 1.

Over most of the observed trail the flicker is within the range of 100 to 300 cycles per second. In a sense, it follows the general light curve with a gentle rise to maximum and a steeper decline. The peak of the fre-

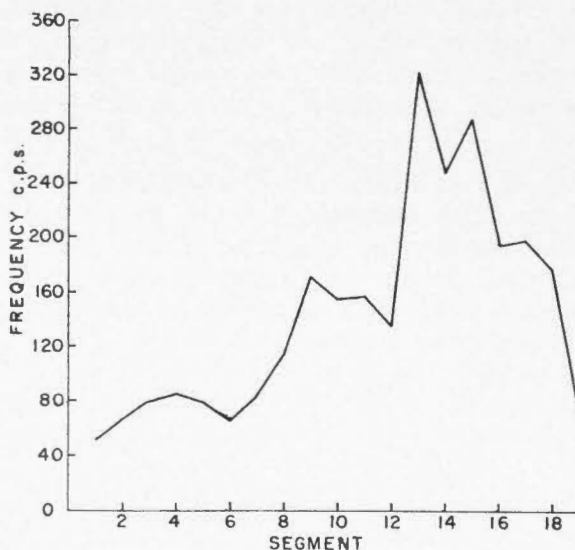


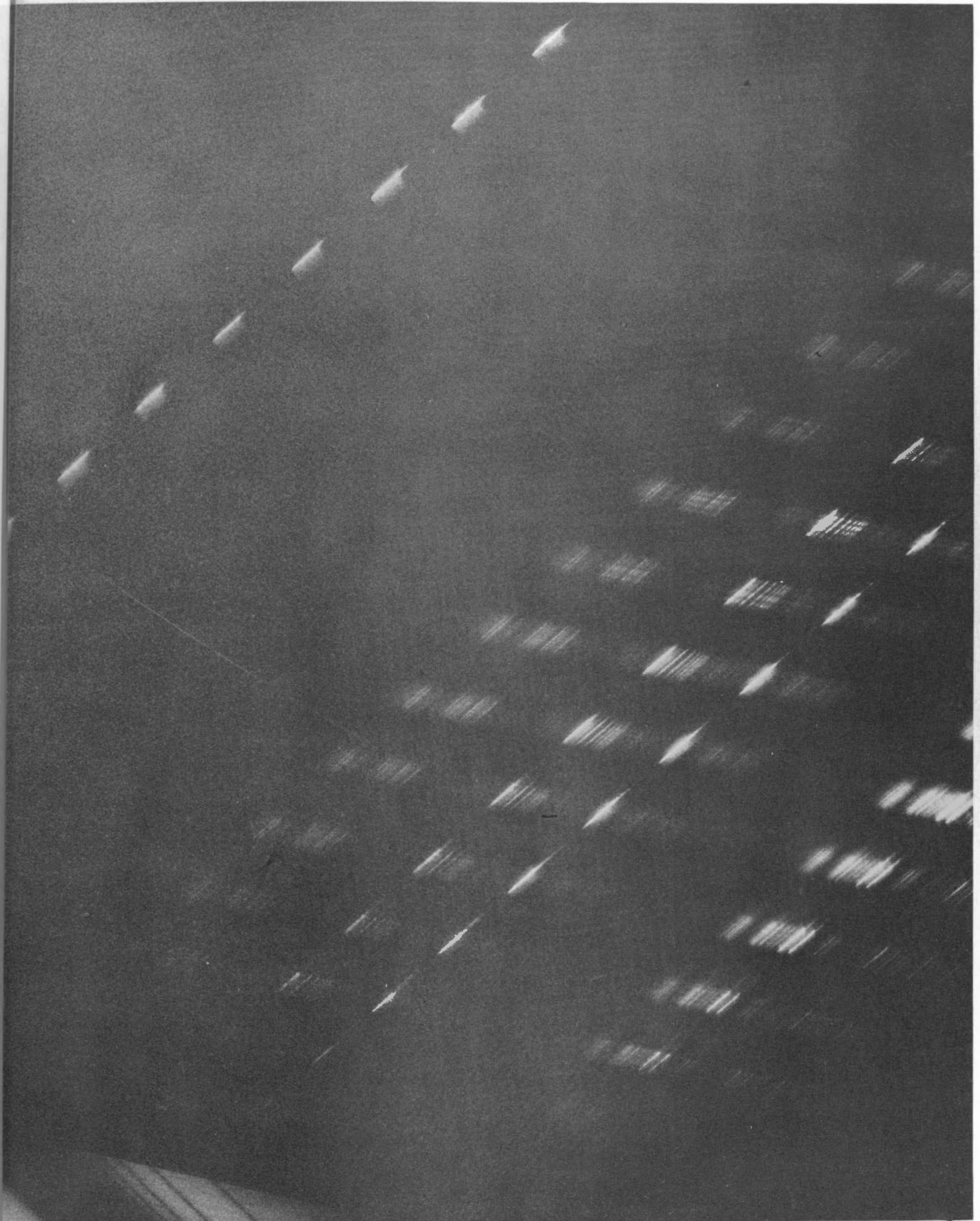
FIGURE 1.—Frequency of the flickering plotted against position along the trail as indicated by segment numbers.

quency curve occurs about two segments after the peak of the light curve. From segments 9 to 12 the frequency is fairly constant near 150 cps, but jumps suddenly at segment 13 to about 320 cps and then declines, only slowly, for another two segments. The amplitude of an individual fluctuation reaches a maximum near segments 10 to 12, resulting in a more pronounced fluting of the spectrum here than at other places.

The periodic flaring might be interpreted as indicating the repeated crumbling or fragmentation of minor amounts of material from the main meteoroid in the form of solid fragments. The increased surface area exposed to ablation would then account for the increased luminosity at each minor flare.

Alternatively, the phenomenon might be closely associated with rotation of the meteoroid. If the meteoroid is quite irregular in shape and rotates in such a manner that it alternately presents a large side and a smaller end to the oncoming atmosphere, then the amount of material ablated, in gaseous form, would vary in a periodic manner. The light, of course, is produced by the hot ablated gas and not by the solid surface.

A third possibility, suggested by Dr. L. G. Jacchia, is based on laboratory studies of ultraspeed pellets by Rinehart (Rinehart, Allen, and White, 1952). A flashing phenomenon was observed for the pellets and explained by an oscillation of the pellet during its flight. The luminosity will be low if there is a leading edge of the object, and high when a whole face of the object is exposed to ablation. For a meteor at relatively low heights where continuum flow occurs, as is expected for this Geminid, an oscillation may be set up that would lead to a flickering phenomenon. Sudden jumps in the frequency of the flicker, such as are observed near segment 8 and again just before segment 13, could indicate a tumbling of the meteoroid to oscillate about a new axis. On the rotation hypothesis these changes might be interpreted as a fracturing of the object into two or more pieces with an accompanying increase in rotational velocity for each piece. It is noted, however, that no general increase in luminosity accompanies these changes in the period of the flicker,



8

9

10

11

12

13

14

15

16

17

18

PLATE 1

A Geminid meteor spectrum showing parts of the zero order (at left), and first- and second-order spectra. Segment numbers are indicated at right.

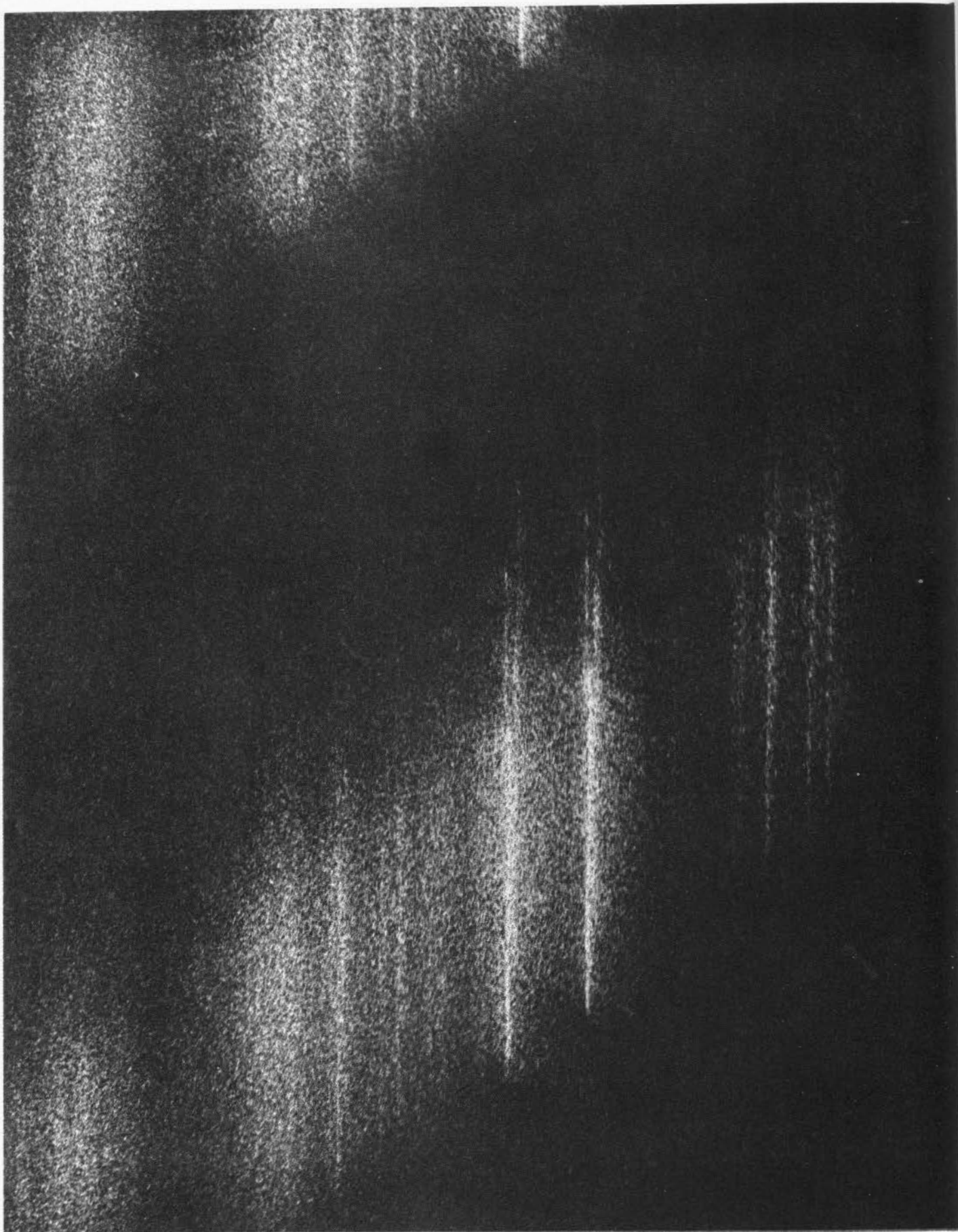


PLATE 2

Greatly enlarged portion of the meteor spectrum showing the split wave-lines of H and K in segment 15 of the second-order spectrum.

which suggests that the effective exposed area is not greatly changed. This would appear to favor the oscillation hypothesis.

The wake spectrum

The zero-order image shows a slight wake in the gap between the segments, beginning at segment 6. The D lines of Na I show a strong wake where they enter the field of the camera at segment 11, and the wake is observable as far as segment 19. Peak intensity of the wake occurs at segment 15, where the following multiplets can be detected in the wake: Na I, 1; Mg I, 2, 3; Ca I, 2; Ca II, 1; Mn I, 2; Fe I, 1, 2, 4, 5, 15, 20, 21, 41, 42, 43.

Most of these multiplets have been listed in earlier studies of wake spectra (Halliday, 1958), although the manganese lines near 4030 Å have not been listed previously. The wake spectrum shows the usual preference for lines of low excitation potential, but it is less pronounced than in most other cases. The line of Mg I, 2 at 5183.6 Å is moderately intense in the wake, whereas its presence was quite doubtful in most earlier wake spectra. The H and K lines of Ca II are strong in the wake and persist essentially as far back into the gap as the other wake lines, in contrast to some spectra in which the H and K lines decay much faster in the wake than the low-excitation Na I and Fe I lines.

The most significant feature of this spectrum appears to be a clear splitting of the stronger wake lines into two components. It is observable in the second-order spectrum from segments 14 to 18. The H and K lines show the splitting most distinctly because of their strength, but other lines in which it is also observable are: λ 4045 of Fe I, 43; λ 4226 of Ca I, 2; and λ 4383 of Fe I, 41. For the Na D lines, in the first-order spectrum, the situation is complicated by the fact that the splitting is in general comparable to the separation of the two D lines. In segments 18 and 19, however, the separation due to the splitting effect is large enough to show in spite of the duplicity of the spectral feature. For the remainder of the wake lines the intensity in the wake is either too low or the resolution of individual lines is too poor to identify both components of the wake lines.

The two components of one wake line may be considered as "red" and "violet" compo-

nents; i.e., displaced to longer or shorter wavelengths compared to the position of the main spectral line in the adjacent segment of the normal meteor spectrum. The flickering effect can be detected in the wake, although in some cases only one component appears to strengthen. The individual components show distinct curvature in places with little correlation between the two components. In some instances the wake components can be traced down the trail well into the following segment of the meteor spectrum.

Individual descriptions of the components of the H and K lines, in the second order, are given below for segments 14 to 18.

Segment 14.—The red component is the stronger, shows some curvature, and appears to fluctuate more due to flickering than does the violet component. The images are within 1 mm of the extreme edge of the plate, which limits the value of this segment.

Segment 15.—A large-scale reproduction of this region is shown in plate 2. The red component is strong near the main segment and can be traced back farther than the violet one. The effects of flickering are more evident in the violet component. Both components show some minor kinks, particularly near the main segment.

Segment 16.—The red component is very strong in the lower portion of the wake, while the violet component is weak. The violet line strengthens considerably at an earlier flare in this segment of the wake. The red component may be detected higher than the violet one, and also continues about two-thirds of the way through the main part of segment 16. With decreasing height within the segment, the red component approaches the main line but fades out before actually joining the main spectral line.

Segment 17.—The violet component is much the stronger in this segment. Just above the main segment the splitting is quite large, while the violet line bends over toward the red component a little farther up in the wake.

Segment 18.—The wake is now quite weak, with the violet component stronger than the red component. The splitting of the two components is larger than in earlier segments.

In the first-order Na D lines the two components are not clearly resolved until segment 18. Faint double wake-lines are also detectable in segment 19 for Na D, with an even wider separation than in segment 18.

Interpretation of the double lines

One obvious explanation to consider for the doubling of the spectral lines in the wake is a physical splitting of the meteoroid into two pieces. This has been observed for some meteors; for example, in spectrum 132 (Millman and Cook, 1959). A splitting of the meteoroid was suggested as one possibility to account for the sudden jump in the frequency of the flicker at segment 13. While this may have occurred it is not the explanation for the double wake-lines, since the wake-lines are generally converging near their lower ends in each segment, while a splitting of the meteoroid would lead to diverging fragments. In segment 16 the red component can be traced for a total distance equivalent to half a complete segment, whereas the exposure time is only one-third of a segment; i.e., the red component is not an exposure on a trailing fragment.

The two components are not due to Doppler effects of an expanding column. The observed splitting would correspond to a relative expansion, transverse to the direction of meteor motion, of about 600 km/sec. This is a most unreasonable value when the initial velocity of the meteor was only 36 km/sec.

The best interpretation is that the wake represents a time exposure of the expanding column of meteoric gas, taken while the luminosity is decaying. Meteor spectrographs are slitless spectrographs, which produce a broad image of a broad source even in monochromatic light. The two wake components apparently represent a side view of a hollow luminous column that shows two well-defined edges because the effective thickness of the luminous portion is small compared to the thickness of the entire column. Note that in comparing the two components at a particular point on the trail, one should compare two points on a line perpendicular to the direction of meteor motion, rather than two points on a line parallel to the spectral dispersion.

Figure 2 shows three computed curves for the intensity profile plotted along a radius of the column from $x=0$ at the center to $x=1.0$ at the outer edge. The three curves correspond to an effective thickness t of the luminous portion of the column of 0.05, 0.15, and 0.40, in units of the column radius. The resolution of the plate is insufficient to rule out very small values of t , but the components are sharp enough to indicate that the effective value of t is not much greater than 0.15.

One complete segment corresponds to $0^{\circ}080$, made up of an exposure of $0^{\circ}027$ and an occulted interval of $0^{\circ}053$. The wake is observable approximately halfway across an occulted portion, from which it follows that the effective duration of the luminosity is considerably less than one shutter break. For all points within the gap, the total exposure is the same, $0^{\circ}027$, but the "age" of the column when the exposure starts is different for each point. A point at the lower end of a normal wake, where the main meteor spectrum segment is starting, receives an exposure from age $t=0^{\circ}0$ to $t=0^{\circ}027$. For a point in the middle of the gap, the exposure runs from $t=0^{\circ}027$ to $t=0^{\circ}054$. This is about the last observable point in most segments; i.e., there is insufficient luminosity emitted after $t=0^{\circ}03$ to record on the plate.

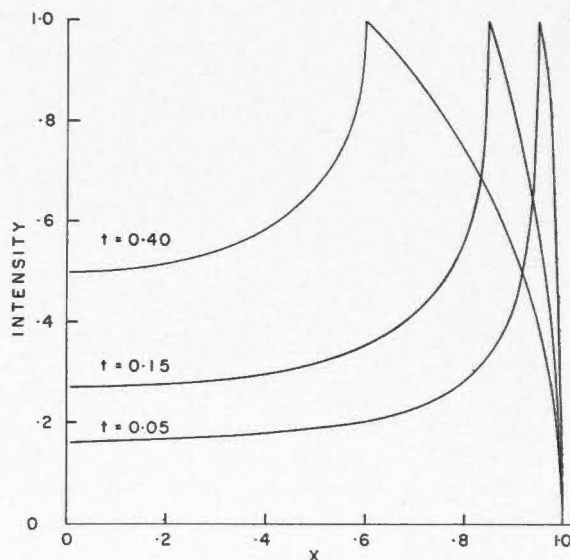


FIGURE 2.—Computed intensity profiles for three values of t , the effective thickness of the luminous column.

As noted earlier, some of the wake lines, particularly the red components, can be traced down into the following segment. For different points within the segment itself, all exposures start at $t=0$ but have different durations. The durations decrease linearly with distance down the segment from a maximum exposure of 0^o027 at the top to 0^o000 at the bottom (where the shutter occults the camera for the next 0^o05). In segment 16, it was noted that the red component was observable two-thirds of the way through the segment; i.e., for any exposure duration longer than 0^o009.

Magnitude of the splitting

Once it is known that the split lines correspond to a physical separation of material in the meteor column, it becomes of interest to determine the magnitude of the splitting. The separation of the two components was measured at frequent intervals in each segment of the wake, and the results were plotted. The scales were converted to diameters of the column, in meters, by allowing for the plate scale and the range of the meteor corresponding to each segment.

The results are presented in table 3, where the curves have been read at equal intervals corresponding to 0^o004 of meteor travel. For example, a time of $t=0^o012$ indicates a point in the occulted portion from which it took the meteor 0^o012 to reach the point at which the shutter reopened to begin the next segment of the main spectrum. (The entire gap corresponds to 0^o053, and although the wake can sometimes be detected at least halfway through the gap, both components are seldom observable for more than one-third of the gap.) The mean splitting within each segment is shown at the bottom of the table.

TABLE 3.—Diameters of the column (meters)

<i>t</i> (sec)	Segment				
	14	15	16	17	18
0.000	----	31	49	69	78
0.004	37	34	49	73	82
0.008	42	39	44	61	85
0.012	----	45	49	54	83
0.016	----	----	53	----	77
0.020	----	----	----	----	77
Mean	40	37	49	64	80

In segments 15 and 16, the red components can be traced into the main segment. They begin with separations from the main spectral line (corresponding to a *radius* of the column) of about 24 meters. One-third of the way down through the segment the separation is about 16 meters, and this is maintained for another third of the dash, until the line fades out as noted previously. At the lowest observable points these red components are displaced about 16 meters from the main column, recorded in an exposure which lasted for only 0^o009.

In all cases where separations for lines of Ca I or Fe I could be measured, the observed points fell quite well on the corresponding curve derived for the H and K lines of Ca II.

The splittings within one segment of the wake are fairly constant; i.e., the red and violet components are nearly parallel. The mean values for the five segments show a curious dependence on height: the splitting increases with decreasing height and may be represented quite well by the linear relation

$$d = 550 - 9.41 h,$$

where d is the diameter in meters at a height of h km. The relation is derived from observations between heights of 50 and 55 km.

From the observed rates of expansion, one may compute an equivalent diffusion coefficient. Öpik (1958) has shown that an effective radius R at time t may be defined by $R^2 = 3Dt$. For the lowest observed points on the red components, $t=0^o009$, $R=16$ meters, from which $D=9.5 \times 10^7$ cm²/sec. The effective value of t should really be smaller, or D should be somewhat larger. For a typical point in the wake, $R=30$ meters, and an effective value of t is about 0^o03, from which $D=1.0 \times 10^8$ cm²/sec. Öpik tabulates normal diffusion coefficients for these heights of about 2×10^2 cm²/sec; i.e., the observed expansions exceed those predicted from normal diffusion by a factor of 5×10^5 .

Discussion

At the low heights of this meteor one should expect a shock front to form around the moving meteoroid. The observed wake luminosity, however, is produced by meteor atoms of calcium, sodium, and iron, not by atmospheric particles. An effective front of expanding me-

teoric material appears to exist inside the heated volume produced by the shock front. Violent collisions at the surface of this meteoric front continue to excite the meteoric atoms for intervals up to about 0^o03. As shown earlier, the sharpness of the two components of the strong wake lines indicates that the effective thickness of the luminous portion of the meteor column is not more than about 15 percent of its radius, or else the lines would appear more diffuse.

The wake components indicate a diffusion of meteoric material into the atmosphere, but the effective diffusion coefficients are so large as to suggest the phenomenon is essentially explosive. During the initial stages the diameter of the column is observed to expand at a rate in excess of 3 km/sec. It is not surprising that the expansion should be very rapid compared to normal diffusion since the amount of material deposited by such a bright meteor is so great as to constitute a major change in local density along the meteor trajectory. The rate of diffusion of meteoric material in this case is so great that it seems reasonable to infer that much fainter meteors, perhaps any meteor brighter than 0 magnitude, will also give rise to appreciably more rapid diffusion than is observed by radar for faint meteors. Great care should be taken, then, that normal diffusion coefficients are not considered as a known quantity in calculations involving the gas columns left by bright meteors.

It is of considerable interest to note that the ion column of Ca II ions expands at the same rate as the atom column of Ca I or Fe I. This is not normally considered to be the case, at least for radar observations, which, of course, are for meteors about 10 magnitudes fainter than this Geminid. Manning (1958), for example, quotes Loeb (1934) to support a statement that the ion column will diffuse only one-fifth as fast as the atom column. Loeb's results are based on experiments in which ions were allowed to diffuse through an electric field. He states (p. 548): "the velocity gained from the field between impacts is further supposed small compared with the thermal velocities of agitation." It is not clear that these results are applicable to the meteor case, where the presence of an electric field is unlikely and the systematic velocity of the meteor particles is

very large compared with thermal velocities. Manning mentions that the ion column for a bright meteor may be larger than for a faint one if ionization can still be accomplished during the expansion of the atom column. For calcium, 6.09 ev are required for ionization, which is higher than the excitation of any wake line. This makes it more likely that an ion of Ca II, which emits H or K radiation 0^o03 after the passage of the meteor, survived nearly all of that interval as an ion, and was then excited with an additional 3.1 ev to radiate, rather than that the ion was formed from a Ca I atom and excited to radiate by any collision occurring later than perhaps 0^o002 after the atom left the meteoroid.

Rapid rotation or oscillation for this meteoroid is suggested by the regularity of the flickering phenomenon and is supported to some extent by the split wake-lines. The variation in relative intensity between the red and violet components could arise from either mechanism, since varying amounts of material would be ejected from the meteoroid in a manner which is not radially symmetrical. This could also account for some of the curvature observed in the wake lines.

One Perseid spectrum is known which shows a similar but much less pronounced splitting of the wake-lines. It is spectrum 223 in Millman's (1958) list of meteor spectra. The splitting is evident in one segment of the H and K lines, but it is confined to a very short path length near a bright flare. The fact that the phenomenon is so pronounced for the Geminid meteor may be associated with its low height in the atmosphere. The much smaller mean free path may tend to localize the zone where appropriate collisions may occur and effectively shield the inner portion of the wake column, giving rise to the hollow-tube effect.

References

- COOK, A. F., AND MILLMAN, P. M.
1956. Photometric analysis of a spectrogram of a Perseid meteor. *Astrophys. Journ.*, vol. 124, pp. 476-477.
- HALLIDAY, I.
1958. Meteor wakes and their spectra. *Astrophys. Journ.*, vol. 127, pp. 245-252.
1961. A study of spectral line identifications in Perseid meteor spectra. *Publ. Dominion Obs. Ottawa*, vol. 25, pp. 1-16.

- LOEB, L. B.
1934. Kinetic theory of gases. Ed. 2. McGraw-Hill Book Co., New York.
- MANNING, L. A.
1958. The initial radius of meteoric ionization trails. Journ. Geophys. Res., vol. 63, pp. 181-196.
- MILLMAN, P. M.
1954. A provisional list of the major meteor showers. Journ. Roy. Astron. Soc. Canada, vol. 48, pp. 193-195.
1958. Photographic meteor spectra (appendix 6). Journ. Roy. Astron. Soc. Canada, vol. 52, pp. 275-276.
- MILLMAN, P. M., AND COOK, A. F.
1959. Photometric analysis of a spectrogram of a very slow meteor. Astrophys. Journ., vol. 130, pp. 648-662.
- ÖPIK, E. J.
1958. Physics of meteor flight in the atmosphere. Interscience, New York.
- RINEHART, J. S.; ALLEN, W. A.; AND WHITE, W. C.
1952. Phenomena associated with the flight of ultra-speed pellets. Part 3. General features of luminosity. Journ. Appl. Phys., vol. 23, pp. 297-299.

Abstract

A study is made of an unusual Geminid meteor spectrum, photographed between heights of 73 and 47 km. Peak luminosity, estimated at magnitude -8 , occurred near 59 km. The meteor exhibited a pronounced flicker, with a frequency varying from 50 to 300 cycles per second. The flicker may be associated with rotation or oscillation of the meteoroid.

A prominent wake spectrum was photographed between 50 and 55 km, consisting of lines of Na I, Mg I, Ca I, Ca II, Mn I, and Fe I. The stronger lines are split into two distinct components attributed to a hollow luminous column rather than splitting of the meteoroid or Doppler effects. The diameter of the column varies from 40 to 80 meters, but shows no variation from one atom or ion to another. Diffusion coefficients computed from the observed rate of expansion exceed the normal values at these heights by a factor of more than 10^5 . The expansion in this case might be considered as explosive.